LASER INTERFEROMETER GRAVITATIONAL WAVE OBSERVATORY
- LIGO -
CALIFORNIA INSTITUTE OF TECHNOLOGY
MASSACHUSETTS INSTITUTE OF TECHNOLOGY

Technical Note	**LIGO-T1000294-v1**
Lock Acquisition Study for Advanced LIGO	
L. Barsotti, M. Evans	

This is an internal working
note of the LIGO project

California Institute of Technology
LIGO Project, MS 18-34
Pasadena, CA 91125
Phone (626) 395-2129
Fax (626) 304-9834
E-mail: info@ligo.caltech.edu

Massachusetts Institute of Technology
LIGO Project, Room NW17-161
Cambridge, MA 02139
Phone (617) 253-4824
Fax (617) 253-7014
E-mail: info@ligo.mit.edu

LIGO Hanford Observatory
Route 10, Mile Marker 2
Richland, WA 99352
Phone (509) 372-8106
Fax (509) 372-8137
E-mail: info@ligo.caltech.edu

LIGO Livingston Observatory
19100 LIGO Lane
Livingston, LA 70754
Phone (225) 686-3100
Fax (225) 686-7189
E-mail: info@ligo.caltech.edu

WWW: http://www.ligo.caltech.edu/

1 Introduction

The lock acquisition strategy presented here is being designed in order to reach the operating point in a deterministic way and in a short time (not longer than a few minutes). In other words, we want a technique which is robust, fast and easy to implement. In this section results for lock acquisition of a broad-band signal recycled IFO are presented. Once the IFO is locked in this configuration, the operating point for the detuned case can be reached by changing continuously the control scheme.

2 Optical Configuration

The optical parameters adopted (see Table 1) are slightly different with respect to the ones proposed at the beginning of this document, but no significant differences in the interferometer response are expected.

Quantity	**Value (Final design value)**
Arm Finesse	621 (446)
ITM transmission	0.010 (0.014)
PRM transmission	0.0318 (0.027)
SRM transmission	0.19 (0.2)
Schnupp asymmetry	0.043 (0.05)
l_{PRC}	55.815 m
l_{SRC}	9.563 m (57.410 m)
l_{EX}	3994.75 m
l_{EY}	3994.75 m
Lower mod. frequency (f1)	$9,399,566$ Hz
Upper mod. frequency (f2)	$46,997,832$ Hz
Modulation index (f1, f2)	0.2

Table 1: Optical parameters adopted in the lock acquisition simulation. The current values chosen for Advanced LIGO, when different, are reported in parenthesis.

3 Sensing and Control

The overall locking path is as follows: by means of an arm length stabilization system (ALS, [3]), the locking sequence starts with the arm cavities locked away from resonance, with the CARM d.o.f. detuned by about 10 nm with respect to the operating point. The d.o.f's of the central cavity (PRCL, MICH, SRCL) are then locked, so as to have a globally controlled state of the IFO from the beginning of the locking sequence. From this stable state, the IFO

is brought to its operating point by progressively reducing the CARM offset. In order to do this, we have to deal with several problems.

First of all, we need to find a good error signal for CARM in presence of a CARM detuning, when standard Pound-Drever-Hall signals are not good error signals. Moreover, the CARM detuning induces an optical resonance, whose frequency is proportional to the detuning itself (75 Hz/nm). The optical resonance changes therefore its frequency while the CARM offset is reduced. The frequency response of all the signals sensitive to CARM changes as well, and it needs to be compensated in order to have a stable loop over the whole sequence. Good error signals for the central cavity have to be found as well. They need to be as independent as possible from the CARM detuning, to avoid complicating the locking sequence. The error signals investigated for the science mode configuration do not have these features. Suitable error signals have been selected after investigating their behavior by means of the frequency domain simulation Optickle.

In the following paragraph the locking sequence will be described in terms of the CARM offset. Figure 1 gives us an idea of how much power circulating in the IFO is associated with a given CARM offset. It shows the power measured in transmission of one arm cavity of the signal-recycled IFO as function of the CARM offset, normalized with respect to the power measured when PRM and SRM are misaligned (about 60 μW, single cavity configuration). When the IFO is at its operating point, about 1000 times more power is expected to be measured in transmission than the single cavity case.

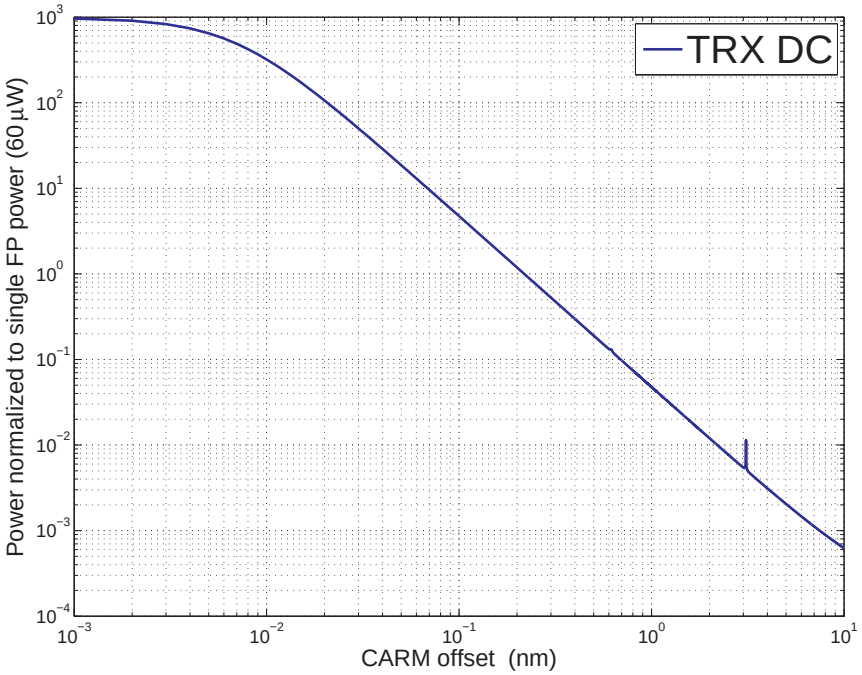

Figure 1: Power transmitted by one arm cavity in signal recycled configuration, normalized by the power measured in single cavity configuration (PRM and SRM misaligned).

3.1 Arm cavity error signals

The use of the power signals transmitted trough the arm cavities as error signals has been investigated, following the strategy adopted in the experimental locking tests carried on at the LIGO-40m laboratory. Figure 2 shows the frequency response to a CARM motion of a combination of the two arm cavities transmitted powers (TRX_DC and TRY_DC), more precisely the square root of the sum. The plot shows the optical resonance in the presence of different values of the CARM offset. The optical resonance frequency moves from several hundred Hz down to a few Hz. For offset values smaller than a few nm, the gain is almost constant above 200 Hz.

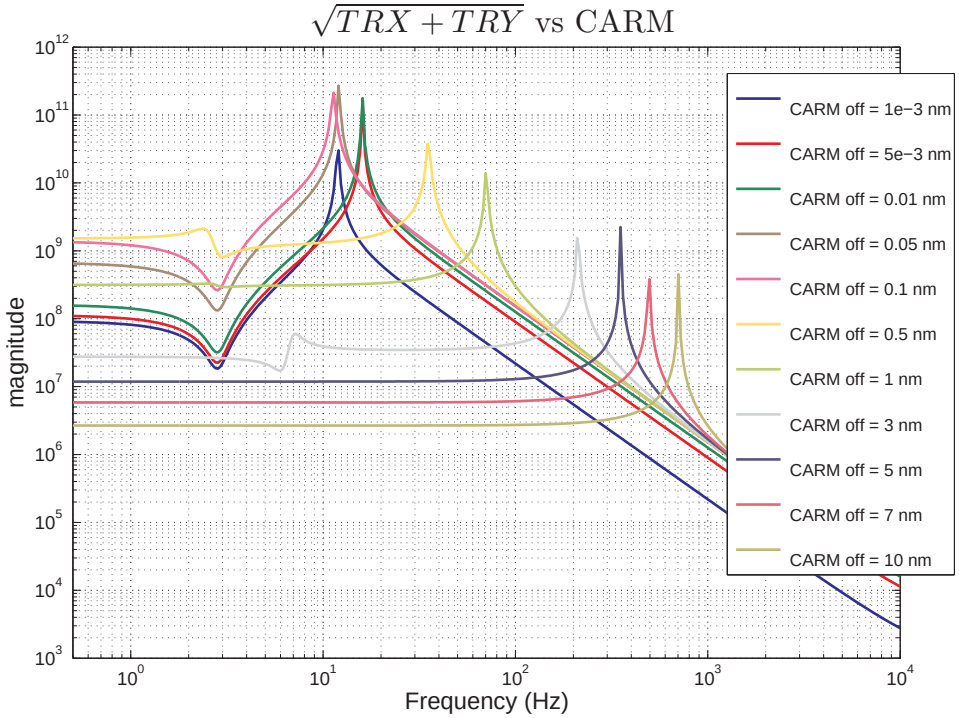

Figure 2: Frequency response of the CARM error signal $\sqrt{(TRX + TRY)}$ to a CARM motion.

Concerning DARM, a good error signal turned out to be the difference between TRX_DC and TRY_DC, with a frequency response which is flat up to a few hundred Hz.

3.2 Central cavity error signals

Standard Pound-Drever-Hall signals generated by the beating between carrier and sidebands and demodulated at the modulation frequency are strongly dependent on the behavior of the carrier inside the arm cavities. These signals are therefore affected by changes of the CARM offset, and they are not useful for controlling the central cavity d.o.f's in our scheme.

Moreover, in broad-band configuration, double demodulation ($f_1 + f_2$, $f_2 - f_1$) does not provide useful error signals for control. In order to get signals which are independent from the CARM offset, the use of signals demodulated at three times the modulation frequency (3f) have been studied. The main features of these signals is that they are produced by the beating between 2f and f sidebands and between 3f sidebands with the carrier. The second contribution is typically smaller than the first one, so that the 3f signal depends very little on the carrier behavior. Signals detected in reflection and demodulated at $3f_1$ and $3f_2$ are in fact very good signals for PRCL, MICH and SRCL, as shown in figure 3. For different values of the CARM offset, the behavior of a 3f-demodulated signal is compared with the single f-demodulated signal planned to be used in science mode. Where the f-demodulated signal is strongly dependent on the CARM offset, the 3f-demodulated signal is almost independent.

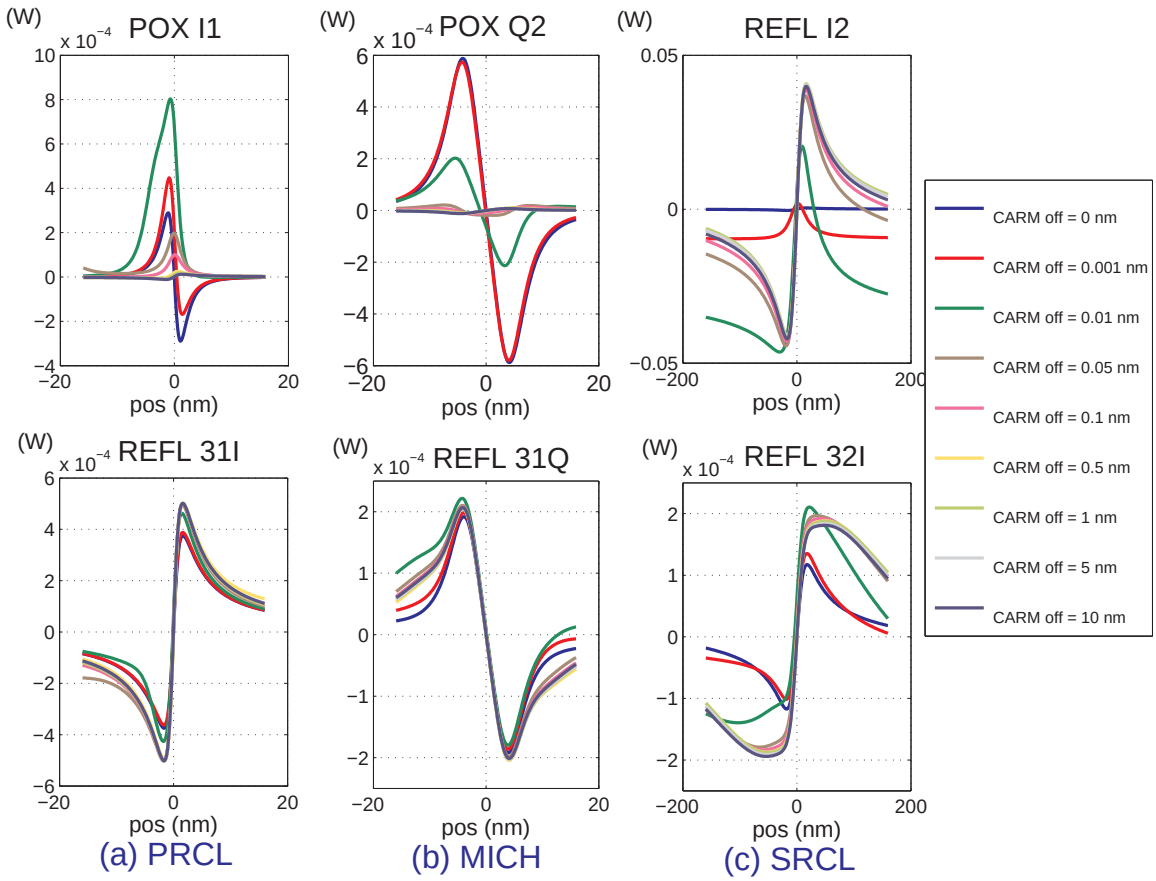

Figure 3: Error signals for PRCL, MICH and SRCL, plotted at different CARM offsets: (top) signal planned to be used in science mode; (bottom) signal 3f-demodulated. REFL 31 means signal extracted in reflection demodulated at the frequency $3f_1 \sim 28$Hz. Similarly, REFL 32 means demodulation at $3f_2 \sim 141$Hz. For MICH, both REFL 31Q and REFL 32Q show the same behavior (only REFL 32Q plotted here).

The resulting control scheme for lock acquisition is shown in Table 2.

Control filters for each degree of freedom are plotted in figure 8.

D.o.f	Error signal	Driven Mirrors
CARM	$\sqrt{TRX + TRY}$	Frequency servo
DARM	$TRX - TRY$	ETMX, ETMY
PRCL	REFL 31I	PRM
MICH	REFL 31Q (or REFL 32Q)	BS, PRM, SRM
SRCL	REFL 32I	SRM

Table 2: Summary of the error signals used to control each d.o.f during lock acquisition, and the mirrors driven by the relative correction signals.

4 Time domain simulation of lock acquisition

A time domain simulation based on the E2E model has been developed in order to test the designed control scheme for lock acquisition. The main features of the simulation are the following:

- simplified suspensions (double pendulum for BS, simple pendulum for the other mirrors);
- saturation of the end mirror actuators at 200 μN (Electrostatic Drive limit), saturation at 10 mN for PR and SR (standard LIGO I actuators), 600 mN for BS (actuation from the penultimate mass);
- shot noise, electronic noise (see section 5.1 for details).

Lock acquisition with full power entering the IFO (125 W) would be complicated by by radiation pressure and thermal effects, so we plan to acquire the lock with a lower incoming power, which will be then brought to its nominal value once both longitudinal and angular controls are active. This simulation uses 1 W of incoming power, and assumes therefore that radiation pressure and thermal effects are negligible. A proper simulation of the ALS system is not present yet. Its behavior is approximated by setting the initial position of the end mirrors so as to have both DARM and CARM offsets of a few nm, then sweeping the end mirrors to reduce the CARM offset. The central cavity is locked when the arm cavities are away from resonance, and remains stably locked during the CARM offset reduction. When the transmitted power of one of the two arms goes above a given threshold, that arm is locked by using the transmitted power as an error signal. The threshold is set at about 30μW, which corresponds to half of the transmitted power in single cavity configuration. This power level can be easily reached by reducing the CARM offset with the ALS given less than a 3 nm initial offset for DARM. Since the ALS will provide an accuracy better than 1 nm on the mirror positions, this requirement is not stringent. As soon as the transmitted power of the second arm goes above the threshold, a common and differential control of the two cavities is engaged, according to the control scheme described in table 2. The DARM control is done by fed-back to the end mirrors. The CARM d.o.f. is instead expected to be controlled by feed-back to the laser frequency, with an initial loop bandwidth of about 200 Hz

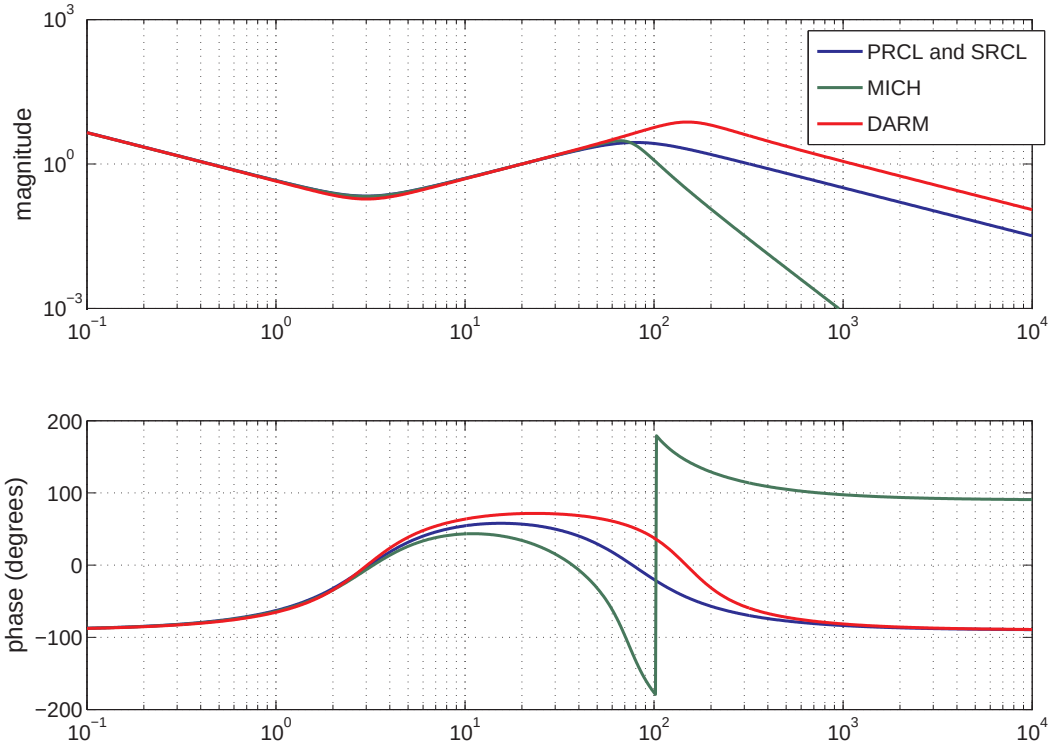

Figure 4: Control filters for DARM and the central cavity degrees of freedom. The corrections sent to the BS are further filtered in order to compensate for the double pendulum in the penultimate mass to mirror mechanical transfer function. The frequency servo is described in section 4.1.

(see section 4.1). From this globally controlled state, the CARM offset is then progressively reduced. The final step of lock acquisition consists of moving the control of the arm cavities from DC to RF signals (REFL I1 for CARM and AS Q2 for DARM).

Figure 5 shows the full lock acquisition of the IFO.

4.1 Frequency servo

In initial LIGO a globally controlled stable state of the IFO is reached only at the end of the lock acquisition sequence. A frequency servo is engaged when the IFO is already on its final operating point. The feedback to the laser frequency is fully analog, with a bandwidth of about 20 kHz. With the locking scheme described here the IFO is instead brought to the operating point by passing through stable states, which allows the activation of a frequency servo even during lock acquisition. Because of the weakness of the end mirror actuators, controlling CARM by feed-back to the laser frequency (and not to the end mirrors) is much more robust.

Possible strategies for implementing a frequency servo during the locking sequence have

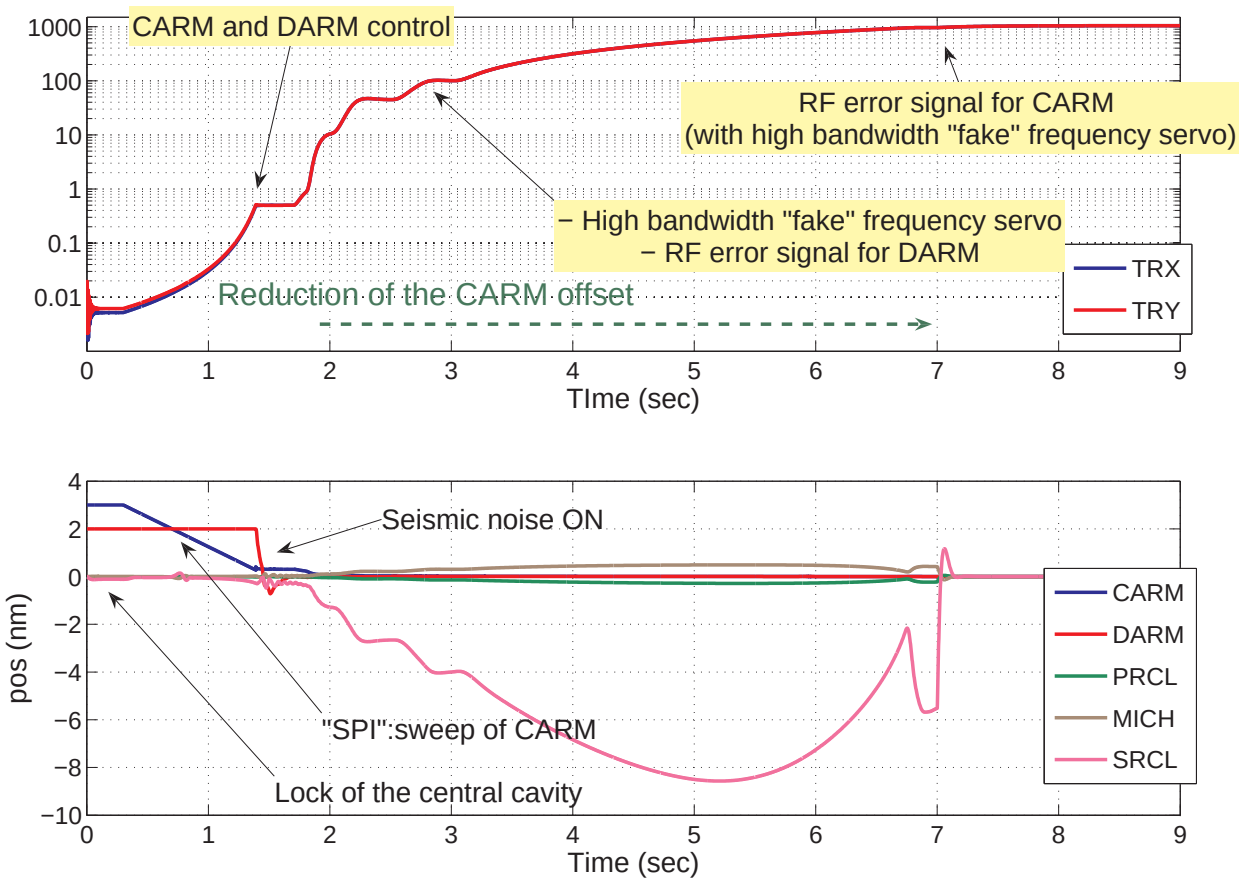

Figure 5: Full lock acquisition sequence.

been studied. The error signal of the frequency servo described in the previous section is a combination of the the arm cavities transmitted powers, TRX_DC and TRY_DC. A few hundred Hz is the maximum loop bandwidth which can be achieved with the current LIGO digital system. A high bandwidth analog frequency servo is likely not to be mandatory for acquiring the lock, but it might turn out to be useful. The implementation of a high bandwidth analog frequency servo using the arm cavities transmitted power as error signal, even if it is possible, would require a non negligible commissioning time because of the kilometric distance between the end stations and the laser. Moreover, for the same reason, not more than a few kHz of bandwidth will probably be achieved. One solution could be the use of the DC signal in reflection from the IFO ($REFL\_DC$), which is sensitive to CARM. Since this signal is nearly AC coupled (as shown in figure 6), another signal would need to be used at low frequency.

A possible implementation, similar to the strategy used to lock the LIGO-40m prototype, is the following:

- beginning of the locking sequence: $\sqrt{TRX + TRY}$ as error signal, digital loop, low bandwidth (∼200Hz);

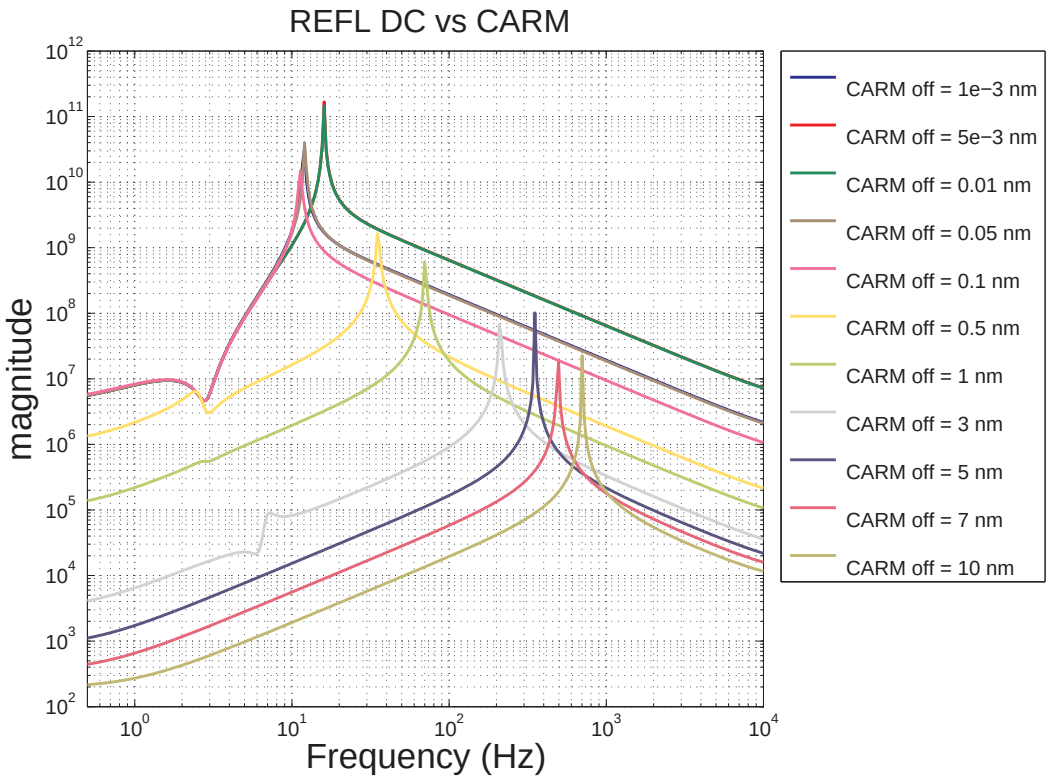

Figure 6: Frequency response of $REFL\_DC$ to a CARM motion.

- during the sequence: combination of $\sqrt{TRX + TRY}$)(digital, DC − 50Hz) and $REFL\_DC$ (analog, 50 Hz - 20 kHz);
- final state: REFL I1 as error signal, analog loop, high bandwidth ($\sim 20kHz$).

This strategy has been tested in simulation. The effect of a frequency servo has been reproduced by a "fake" servo in which the CARM correction signal is sent to the end mirrors by-passing the mechanics and therefore avoiding saturations. In the lock acquisition sequence shown in figure 5, the switch from a low bandwidth to a high bandwidth loop is done when the arm cavity transmitted power is about 100 times the single cavity power. The reason for this is that $REFL\_DC$ does not appear to be very sensitive to CARM in presence of bigger CARM offsets. However, a deep investigation on this point has not been done yet, and a transition at an earlier stage might be possible anyway.

5 Signal Read-Out for Lock Acquisition

The design of signal read-out is typically done in order to produce signals shot noise limited, that is signals in which the read-out noise (amplifier noise, Johnson noise, etc..) is well below the shot noise. However, this constraint is not really necessary during lock acquisition, where

we are not concerned about sensitivity issues. Since the lock acquisition scheme currently designed for AdvLIGO [1] involves signals at quite high frequency (around 140 MHz), it is useful to know the tolerance that we have on the read-out noise in order to possibly simplify the read-out design for lock acquisition. The analysis which follows is done in this way:

- for each photo-detector, the maximum shot noise level $\widetilde{P}_{shot}$ in $W/\sqrt{Hz}$ is computed;
- by assuming the photo-detector to be shot noise limited, and knowing the transfer function from shot noise to actuators, the resulting correction signal shot noise limited is calibrated in $N/\sqrt{Hz}$. As example, figure shows the transfer function from shot noise to actuators for the DARM loop, together with its open loop and closed loop transfer functions and the filter shape;
- the RMS of the correction signal is directly compared with the relative actuator limit: the only requirement that we impose is that the RMS of the correction signals sent to each mirror is at least a factor 10 lower than the mirror actuator limit, in order to be safely far from saturations;
- if the RMS of the correction signal shot noise limited is already only a factor ten lower than the actuation limit, the read-out noise must be lower than the shot noise, otherwise we can afford to have higher read-out noise, as long as the RMS of the correction signal is within the requirement (the read-out noise has the same transfer function to actuators as the shot noise);
- possible read-out topologies currently under investigations for AdvLIGO [2] have been analyzed to see if they would meet the requirement also for lock acquisition.

With a factor 10 margin required with respect to the full range of the actuators, the maximum correction signal (RMS) acceptable on each mirror is summarized in table 3:

Mirror	**Max correction signal (RMS)**
ETMX, ETMY	20 μN
PRM, SRM	1 mN
BS	60 mN

Table 3: Summary of the maximum correction signal (RMS) allowed for each mirror.

The control filters used for the analysis which follows are the ones shown in figure 8. A maximum incident DC power of 10 mW on each diode and a diode efficiency $\eta = 1$, will be considered.

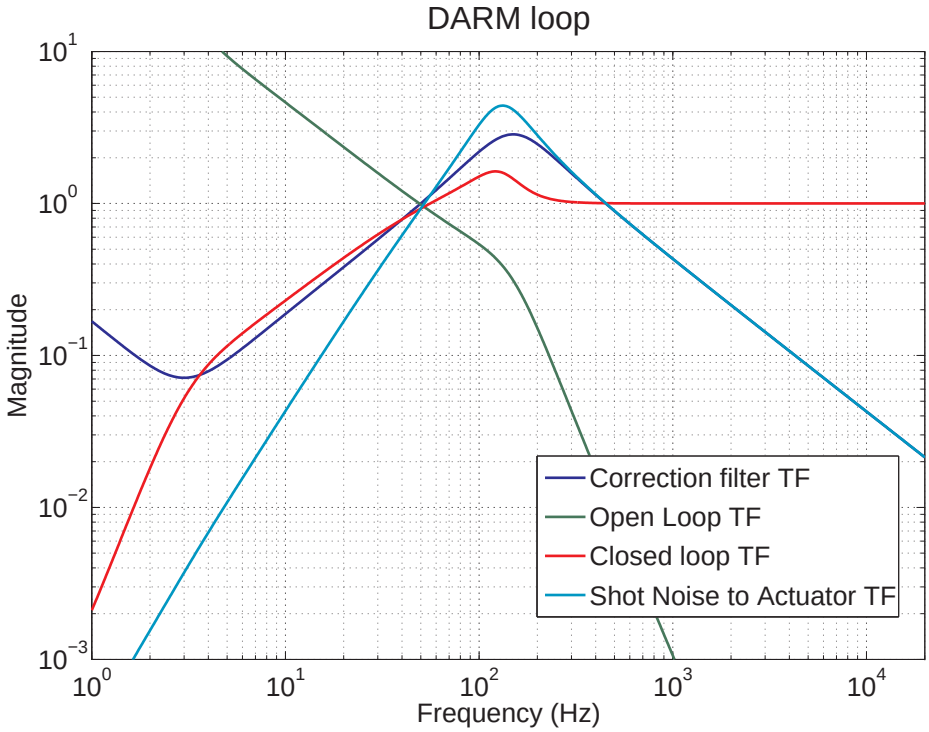

Figure 7: Some transfer function for the DARM loop: filter shape, open loop (unity gain is set around 50 Hz) and closed loop transfer function, and the shot-noise to actuators transfer function, given by the product between the controller filter TF and the closed loop TF (arbitrary unit in the plot).

5.1 Read-out noise requirements

5.1.1 RF Photodiodes at the reflection port: REFL31 and REFL32

Two modulation frequencies are designed for AdvLIGO:

$$f_1 = 9,399,566 \text{ Hz} \tag{5.1}$$
$$f_2 = 46,997,832 \text{ Hz} \tag{5.2}$$

At the reflection port signals are extracted both at $3 \times f_1$ (28 MHz, REFL31) and at $3 \times f_2$ (141 MHz, REFL32). At the beginning of the locking sequence, all the input power is reflected back from the IFO, so that a 99% attenuator is needed on this path in order to have 10 mW on each diode. This condition corresponds to the worse case in terms of shot noise. The power impinging upon the diode is mostly carrier power, which contributes only to increase the shot noise, but not to making signal (produced by the beating between the sideband). The maximum shot noise level, both in power and in current, is therefore:

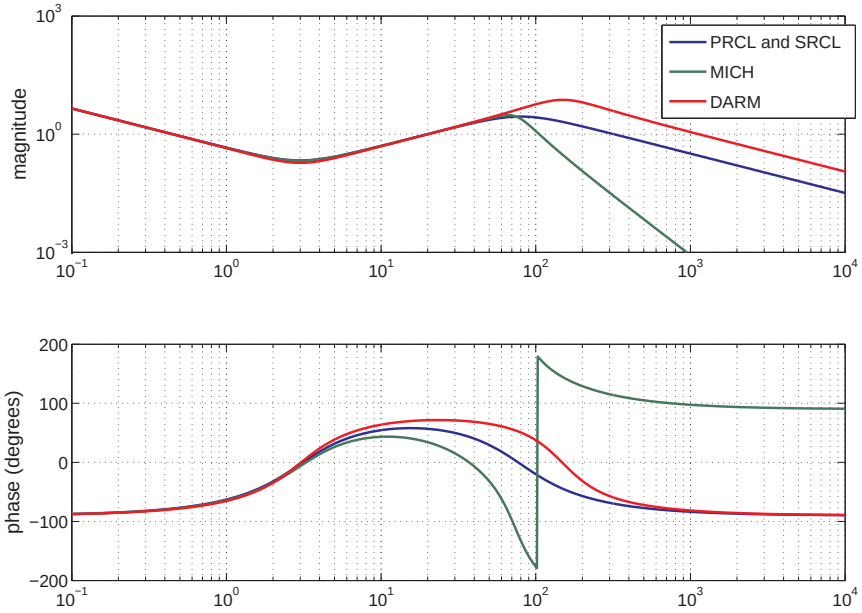

Figure 8: Control filters for DARM and the central cavity degrees of freedom. The corrections sent to the BS are further filtered in order to compensate for the double pendulum in the penultimate mass to mirror mechanical transfer function.

$$\widetilde{P}_{shot} = \sqrt{1 h\nu P_0/\eta} = 4.5 \times 10^{-11} \text{ W}/\sqrt{\text{Hz}} \tag{5.3}$$

$$\widetilde{I}_{shot} = \frac{\eta e}{h\nu}\widetilde{P}_{shot} = 3.6 \times 10^{-11} \text{ A}/\sqrt{\text{Hz}} \tag{5.4}$$

where $P_0 = 10$ mW. The most stringent constraint for setting the requirements on the read-out noise performance of REFL31 and REFL32 is expected to come by the BS control. This is because the actuation for the BS is done from the Penultimate Mass (PM), so an f^3 controller is needed in order to compensate for the PM to mirror transfer function (instead of an f controller). Since the noise is propagated to the mirror through the control filter, this makes the re-injected noise grow by a factor f^2 faster than in the other loops. On the other hand, the BS actuator limit is only a factor 60 bigger than PRM and SRM's one. The possibility of controlling the BS position using both REFL31 and REFL32 is considered in the analysis which follows.

I) REFL31 (MICH controlled by REFL31)

For each mirror of the central cavity, the RMS of the correction signal shot noise limited is shown in table 4.

As said above, the BS actuator limit is 60 times bigger than for PRM and SRM, while the RMS of its correction signal is more than a factor 100 bigger. It is therefore the BS control which sets the requirement for the maximum allowed read-out noise (called generically electronic noise), which can be a factor 15 above shot noise:

Mirror	Corrections shot noise limited (RMS)
PRM:	4.0 μN
BS:	**4.0 mN**
SRM:	14 μN

Table 4: RMS of the correction signal (shot noise limited) sent to each mirror when MICH is controlled by REFL31.

Mirror	Corrections shot noise limited (RMS)
PRM:	2.0 μN
BS:	**1.7 mN**
SRM:	11 μN

Table 5: RMS of the correction signal (shot noise limited) sent to each mirror when MICH is controlled by REFL32.

$$\widetilde{P}_{elect} = 6.75 \times 10^{-10}\ \mathrm{W}/\sqrt{\mathrm{Hz}} \tag{5.5}$$
$$\widetilde{I}_{elect} = 5.40 \times 10^{-10}\ \mathrm{A}/\sqrt{\mathrm{Hz}} \tag{5.6}$$

II) REFL32 (MICH controlled by REFL32)

For each mirror of the central cavity, the RMS of the correction signal shot noise limited is shown in table 5:

With the same argument as before, the maximum electronic noise allowed can be about factor 30 above shot noise:

$$\widetilde{P}_{elect} = 1.35 \times 10^{-9}\ \mathrm{W}/\sqrt{\mathrm{Hz}} \tag{5.7}$$
$$\widetilde{I}_{elect} = 1.1 \times 10^{-9}\ \mathrm{A}/\sqrt{\mathrm{Hz}} \tag{5.8}$$

5.1.2 DC Photodiodes in transmission to the arms: TRX and TRY

DC signals transmitted to the arms are used during lock acquisition. The maximum power on the diodes is achieved at the end of the locking sequence: 31.5 mW. An about 75% attenuator is therefore needed in order to have a maximum power of about 10 mW on the diodes. The signal to shot noise ratio in this case is proportional to the square root of the power impinging upon the diode, so that the worse condition arises at the beginning of the locking sequence, when the power on the diode is the lowest one (about $P_0 = 3.7\mu W$). The shot noise level, both in power and in current, is:

$$\widetilde{P}_{shot} = \sqrt{2hvP_0/\eta} = 1.2 \times 10^{-12}\ \mathrm{W}/\sqrt{\mathrm{Hz}} \tag{5.9}$$
$$\widetilde{I}_{shot} = \frac{\eta e}{hv}\widetilde{P}_{shot} = 9.8 \times 10^{-13}\ \mathrm{A}/\sqrt{\mathrm{Hz}} \tag{5.10}$$

The RMS of the correction signals sent to the end mirrors is 3.4x10^{-6} N. Since the maximum RMS allowed for the end mirrors is 20x10^{-6} N, the maximum photodiode noise allowed can be about factor 5 above shot noise:

$$\widetilde{P}_{elect} = 6.0 \times 10^{-12}\ \mathrm{W}/\sqrt{\mathrm{Hz}} \tag{5.11}$$
$$\widetilde{I}_{elect} = 4.9 \times 10^{-12}\ \mathrm{A}/\sqrt{\mathrm{Hz}} \tag{5.12}$$

5.1.3 RF Photodiode at the anti-symmetric port: AS2

During the locking sequence, when the arm transmitted power is about 100 times bigger than the single Fabry-Perot cavity power, the DARM control is moved form a DC to the RF signal at the second modulation frequency f2, about 47 MHz. The power at the anti-symmetric port is about 4.6 mW. Since this is the gravitational wave signal port, not more than 1% is likely to be available for lock acquisition photodiodes. For this reason, we consider having a power on the diode of about $P_0 = 46\ \mu$W. This power is dominated by the f2 sideband power, since the carrier and the f1 sidebands are not resonant inside the signal recycling cavity, and they are poorly transmitted to the anti-symmetric port. The f2 sideband power is also contributing to make signal, so that the shot noise level, both in power and in current, is given by:

$$\widetilde{P}_{shot} = \sqrt{1.5hvP_0/\eta} = 3.7 \times 10^{-12}\ \mathrm{W}/\sqrt{\mathrm{Hz}} \tag{5.13}$$
$$\widetilde{I}_{shot} = \frac{\eta e}{hv}\widetilde{P}_{shot} = 3.0 \times 10^{-12}\ \mathrm{A}/\sqrt{\mathrm{Hz}} \tag{5.14}$$

The maximum photodiode noise can be up to a factor 3000 above shot noise:

$$\widetilde{P}_{elect} = 1.1 \times 10^{-8}\ \mathrm{W}/\sqrt{\mathrm{Hz}} \tag{5.15}$$
$$\widetilde{I}_{elect} = 9.0 \times 10^{-9}\ \mathrm{A}/\sqrt{\mathrm{Hz}} \tag{5.16}$$

5.1.4 Summary

Table 6 summarizes all the results obtained before.

Photodiode	**Signal**	**Power**	**Shot noise limit**$(\mathrm{A}/\sqrt{\mathrm{Hz}})$	**Max elect noise**$(\mathrm{A}/\sqrt{\mathrm{Hz}})$
REFL 31	RF	10 mW	3.6×10^{-11}	$(\times\mathbf{15})$ 5.4×10^{-10}
REFL 32	RF	10 mW	3.6×10^{-11}	$(\times\mathbf{30})$ 1.1×10^{-10}
TRX , TRY	DC	3.7 μW	9.8×10^{-13}	$(\times\mathbf{5})$ 4.9×10^{-12}
AS2	RF	46 μW	3.0×10^{-12}	$(\times\mathbf{3000})$ 9.0×10^{-9}

Table 6: Summary of the specifications for each photodiode.

6 Conclusion

The lock acquisition strategy for aLIGO, which uses an arm length stabilization system to separate the tasks of locking the arms and the central cavities, has been demonstrated in simulation and will be tested at the LIGO-40m facility. These scheme presented should result in systematic and robust locking for aLIGO.

A Lock Loss

When lock is lost, the energy stored in the arm cavities will exit the interferometer in some uncontrolled way. A number of factors make it likely that there will be challenges associated with power being dumped to the anti-symmetric port:

- the power at the AS port when operating is less than 1W
- essentially all of the AS port power must be detected during operation
- the SRM transmissivity is about a factor of 7 higher than the PRM
- during operation, the SRC is on resonance, while the PRM is anti-resonant
- the arm cavity finesse is much higher than the SRC or PRC, making arm cavity reflection phase likely to change much more rapidly than SRM or PRM reflection phase

The implication of this collection of factors is that as lock is lost the near perfect cancelation of the carrier fields from the arms at the AS port will be lost, while the SRC remains resonant and the PRC remains anti-resonant (as demanded by the signal extraction and power recycling operating point), and thus the majority of the stored energy will exit through the AS port. If nothing is done to prevent it, this can cause the power seen by detectors at the AS port to change by 4 or even 5 orders of magnitude in a few milliseconds. The simulation of an example lock-loss event, in which one end mirror departs from the operating point with a high acceleration ($50\mu m/s^2$), is shown in figure 9.

To set the scale of the discussion, we start by noting that the optical power stored in an aLIGO interferometer operating with 100W of input carrier is roughly 50J. Furthermore, experience from eLIGO indicates that the damage threshold for our photo-diodes is roughly 100mJ. Here we use energy rather than power under the assumption that the time scale on which the energy is delivered is shorter than the dissipative time scale of the PDs, so that the integrated power is more important than the instantaneous power.

Also of note is the arm cavity decay time, which is $3.8ms$ in the absence of signal-extraction, but about a factor of 10 lower when the signal recycling mirror and cavity resonance condition are taken into account. This should be compared with the time required for an arm cavity reflection phase to change by enough to match the Michelson transmission to that of the SRM; about $10ms$ assuming a $400uN$ force and a $40kg$ test-mass. Note that the acceleration show in figure 9 is higher than we expect to be able to generate, and yet the time scale is long compared to the coupled cavity decay time as evidenced by the lack of ringing in the AS port power.

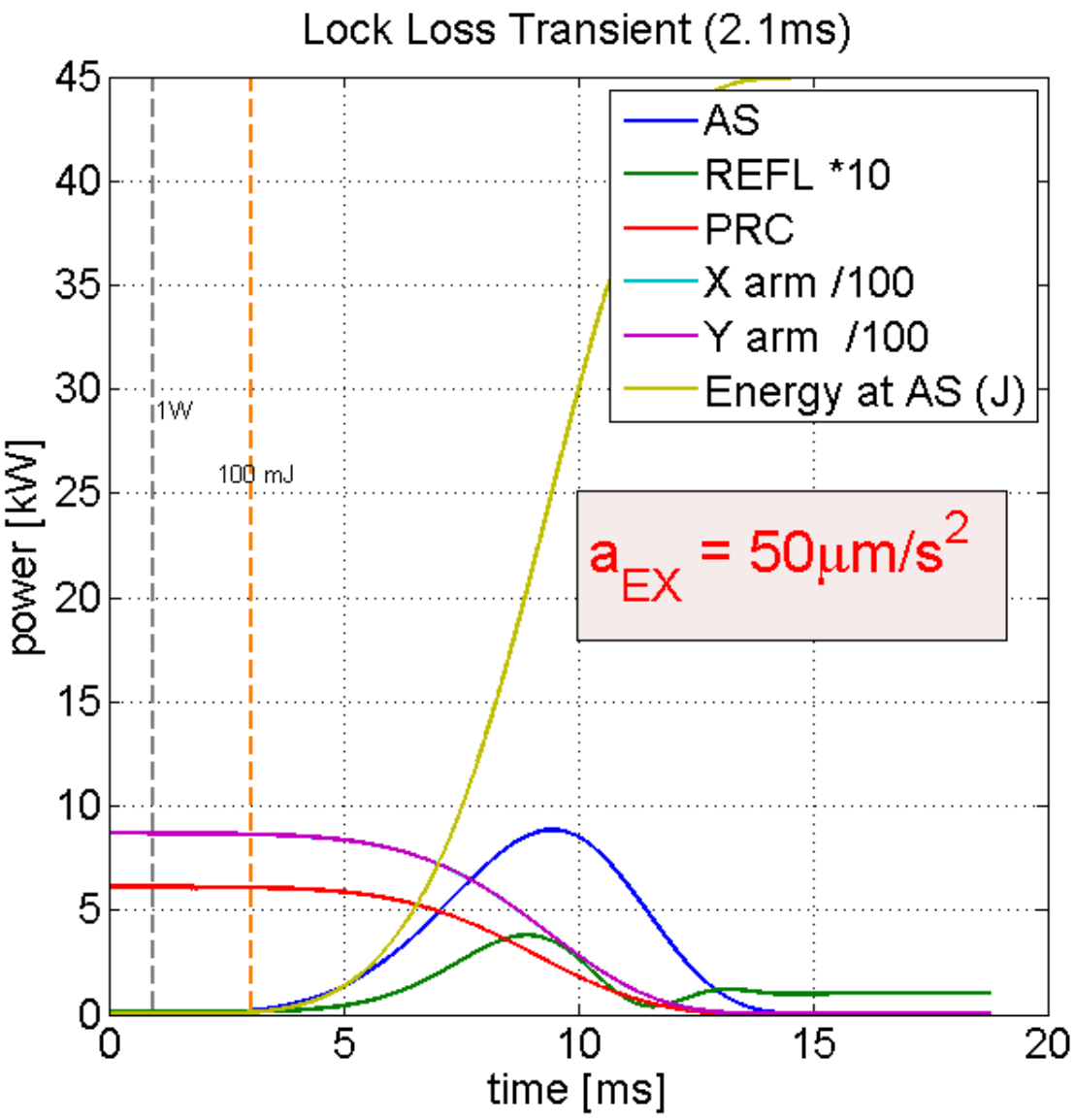

Figure 9: An example lock-loss event. One end mirror departs from the operating point with a high acceleration ($50\mu m/s$) while the other optics do not move.

A.1 Monte Carlo Simulation

To investigate requirements for a shutter capable of preventing damage to the AS port detectors, we developed a Monte-Carlo simulation of interferometer lock loss. In this simulation, the IFO mirrors are given random initial velocities and accelerations chosen from distributions consistent with the force available on each optic (e.g., $10\mu m/s^2$ for the test-masses). The statistic used to summarize the results is the minimum time between crossing an AS port trigger level, for which we used 1 Watt, and the time at which $100mJ$ has been exited the AS port. The times corresponding to the trigger and the damage threshold can be seen in figure 9 as the grey and red dashed vertical lines. The result of the MC simulation is shown in figure 10, where the minimum time between the trigger level and the damage threshold

was found to be $2ms$.

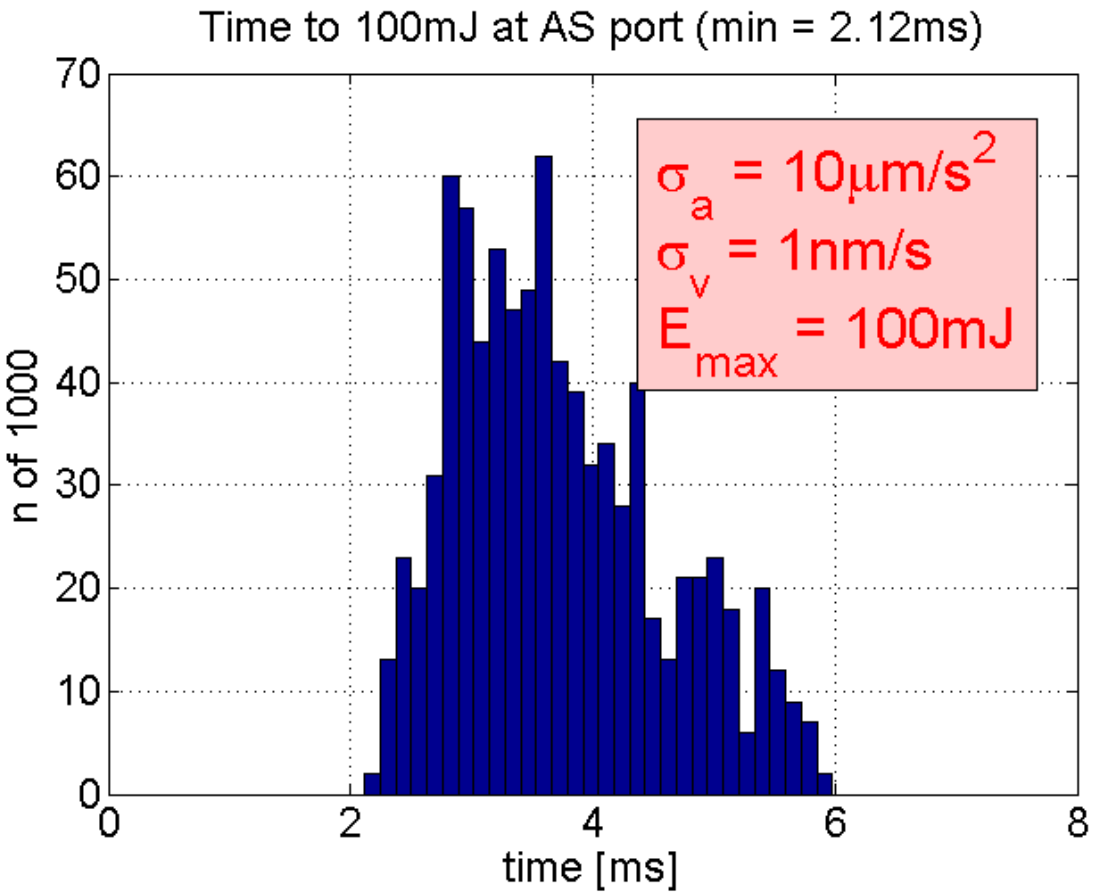

Figure 10: Histogram of time between the trigger level, set at $1W$, and the damage threshold of $100mJ$.

To summarize a few other results found in G1000489:

- If we reduce the damage threshold to $30mJ$, the minimum time reduces to $1ms$.
- Increasing the available test-mass accelerations to $100\mu m/s^2$ also results in a $1ms$ minimum time.
- given the currently planned actuation it does not appear to be possible to move the SRC significantly off resonance in time to prevent damage at the AS port, though the peak AS port power can be reduced.

A.2 Shutter Requirements

To prevent damage to detectors located at the anti-symmetric port during lock loss, we will need to implement a fast shutter. The problem for aLIGO is significantly more challenging than for eLIGO due to both higher stored energy, and shorter decay time. Due to the large

amount of stored energy, we will likely need to protect any PD which receives more than 0.1% of the AS port power.

The main AS port PDs, which receive more than 90% of the power, will need a shutter which is 90% closed in $1ms$ and 99.9% closed in $2ms$. Other detectors, which receive a few percent of the AS port power, will need to be protected on a similar time scale.

References

[1] Rich Abbott et al., *AdvLIGO Interferometer Sensing and Control Conceptual Design*, LIGO-T070247-01-I

[2] Rich Abbott, *RFPD Topology COmparison*, LIGO-T060268-03-C

[3] John Miller et al., *Adv. LIGO Arm Length Stabilisation Design*, T0900144